

Letter

Lattice-Oriented Growth of Single-Walled Carbon Nanotubes

Ming Su, Yan Li, Benjamin Maynor, Alper Buldum, Jian Ping Lu, and Jie Liu

J. Phys. Chem. B, **2000**, 104 (28), 6505-6508 • DOI: 10.1021/jp0012404

Downloaded from <http://pubs.acs.org> on January 1, 2009

More About This Article

Additional resources and features associated with this article are available within the HTML version:

- Supporting Information
- Links to the 6 articles that cite this article, as of the time of this article download
- Access to high resolution figures
- Links to articles and content related to this article
- Copyright permission to reproduce figures and/or text from this article

[View the Full Text HTML](#)



ACS Publications
High quality. High impact.

LETTERS

Lattice-Oriented Growth of Single-Walled Carbon Nanotubes

Ming Su,^{†,‡} Yan Li,^{†,‡} Benjamin Maynor,[†] Alper Buldum,[§] Jian Ping Lu,[§] and Jie Liu^{*,†}

Department of Chemistry, Duke University, Durham, North Carolina, 27708, and Department of Physics and Astronomy, University of North Carolina, Chapel Hill, North Carolina, 27599

Received: March 31, 2000; In Final Form: May 9, 2000

Single-walled carbon nanotubes (SWNTs) with preferred 2D orientations were synthesized for the first time by chemical vapor deposition (CVD) of methane on silicon surfaces terminated with hydrogen, native oxide, and an ultrathin aluminum layer. The SWNTs grown on Si(100)-based surfaces take two perpendicular directions, and those grown on Si(111)-based surfaces take three preferred directions that are separated by 60°. Simulations of SWNTs on Si(100) and Si(111) surfaces indicate that the observed orientation locking is the result of interactions between nanotubes and the surface lattices. The calculated orientations of energy minimums accord exactly with the experimental results and are independent of the tube chirality as observed. In addition, the calculations also show that the (111) surface is stickier than (100), thus explaining the observation that SWNTs grown on Si(111) surfaces are shorter than those on Si(100) surfaces.

Since its discovery in 1991,¹ single-walled carbon nanotubes (SWNT) have been one of the most actively studied materials due to their unique structural, electric properties, and chemical stability.² Experiments showed that individual carbon nanotubes can behave as quantum wires and can even be made into room-temperature transistors.³ These unique electronic properties make nanotubes ideal candidates for components in nanoelectronic devices. However, the integration of single-wall carbon nanotubes to nanometer scale electric devices requires their location and orientation to be controlled to perform desired functions.⁴ For example, to be used as a molecular wire, SWNT must be positioned to link two components of a circuit. Currently, SWNTs were put across two metal electrodes by either random deposition of nanotube suspensions on an array of parallel electrodes⁵ or by manipulating the deposited nanotubes with an atomic force microscope (AFM).⁶ However, these methods

require a large number of attempts and do not have the degree of control desired for making a large number of functional devices. One possible solution for this problem is to synthesize SWNTs with controlled position and orientation directly on a surface, especially on the most widely used silicon surfaces.

MWNTs have been produced on catalyst patterned silicon wafers with their orientations normal to the surface.^{7,8} In addition, SWNTs have been grown on surfaces with random orientation.⁹ However, growth of SWNTs on surfaces with preferred orientation was not reported, except one report of SWNT growth on an AFM tip.¹⁰ In this paper, we report that lattice-oriented SWNTs can be synthesized by chemical vapor deposition (CVD) of methane on hydrogen-terminated silicon surfaces, silicon surfaces terminated with a thin silicon oxide layer, and silicon surfaces coated with a thin layer of alumina. The catalysts can be either individual iron nanoparticles or nanoparticles of an iron–molybdenum mixture. Unlike the vertical orientation within a channel template or on surfaces, we have found that the orientations of SWNT can be determined

* E-mail: jliu@chem.duke.edu.

[†] Duke University.

[‡] Both authors contributed equally to this work.

[§] University of North Carolina.

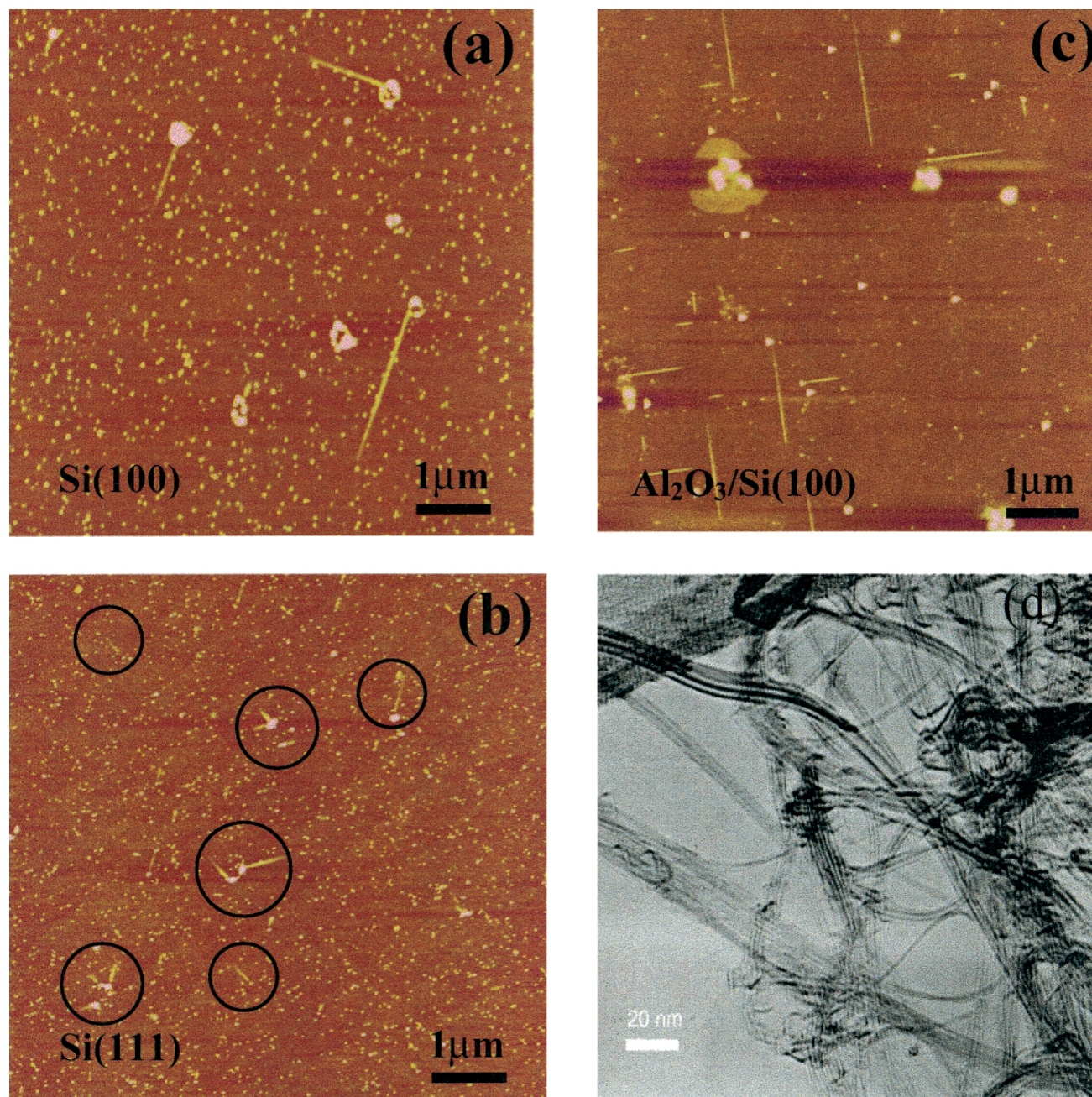


Figure 1. Tapping mode AFM images of SWNTs grown with Fe nanoparticle supported on native oxide layer coated Si(100) surface (a) and Si(111) surface (b), SWNTs grown with Fe–Mo mixed nanoparticle supported on alumina thin film coated Si(100) (c). TEM image of SWNT grown on Fe nanoparticle supported on alumina powder (d).

by the lattice of the substrate, this has both fundamental importance and great potentials in applications.

Silicon wafers used in the experiments were either P type Si(100) or N type Si(111) and used after cleaning by a standard method: First, the wafers were irradiated under UV light in air for 30 min to oxidize organic contaminants on the surface and to form a thin oxide layer, then they were dipped into 1:10 HF aqueous solution to remove the oxide layer and contaminants. After that, the wafers were oxidized again by UV irradiation. Thin film of alumina supported on the silicon wafer was prepared following a reported sol–gel method,¹¹ in which the cleaned silicon wafer was immersed in the solution of $\text{Al}(\text{O}i\text{Bu})_3$ (88 mM) in 2-propanol/carbon tetrachloride ($2/3$, v/v). After 10 min of adsorption, the wafer was washed with 2-propanol and hydrolyzed in water. The adsorption and hydrolysis were both carried out at 45 °C. Samples were then characterized with XPS to confirm the coating of Al_2O_3 .

The iron nanoparticle was synthesized by reducing ferric chloride hexahydrate ($\text{FeCl}_3 \cdot 6\text{H}_2\text{O}$) with lithium borohydride (LiBH_4) in the inverse micelle of didodecyldimethylammonium bromide (DDAB) in toluene.¹² The molar ratio of $[\text{BH}_4^-]:[\text{Fe}_3^{+}]$ was 6:1 in the reaction. The reacted solutions turned black upon reduction, and the nanoparticles formed in the solution were stabilized by surfactant. AFM images of the particles dispersed on mica gave the uniform distribution of particle diameter, which ranges from 2 to 3 nm. The iron–molybdenum composite nanoparticle was synthesized by a similar procedure with a molar ratio of Fe to Mo of 4:1. Typically, 0.054 g of $\text{FeCl}_3 \cdot 6\text{H}_2\text{O}$ was added to 20 mL of 10% DDAB/toluene solution to form the inverse micelles. Then 0.040 mL of 0.1 M $(\text{NH}_4)_2\text{MoO}_4$ aqueous solution was added to the micelle solution under sonication. After that, the solution was bubbled with N_2 to remove dissolved oxygen, followed by adding 0.8 mL of 2.0 M LiBH_4/THF solution to reduce the salts into metals. The

solution turned black immediately upon sonication. The product was then dispersed in 2-propanol, drop-dried on a silicon wafer, and examined with AFM. The diameters of Fe–Mo composite particles are about 2 nm.

The methane chemical vapor depositions are performed in a quartz tube equipped with temperature and gas-flow controls. The samples are first reduced in H_2 for 15 min at 900 °C, then methane (99.99%) was introduced into the system with a flow rate of $1200\text{ cm}^3\text{ min}^{-1}$ for a certain period at 900 °C. After the reaction, methane was replaced by argon and the furnace was cooled to room temperature. SWNTs formed in the CVD process on Si wafers were checked with an atomic force microscope (Nanoscope IIIa, DI) operated in tapping mode, while those grown on catalysts supported on Al_2O_3 powder were characterized with TEM. The diameters of nanotubes grown on Si surfaces range from 0.9 to 2 nm, as measured by AFM. The smaller diameters of nanotubes compared with the starting catalyst particles may be caused by the coating of surfactant on particles. The effect of starting catalyst particle size on nanotube diameter is being studied currently in the group.

As shown in Figure 1, we have observed the growth of carbon nanotubes on catalyst nanoparticles supported on Si surfaces (Figure 1a,b) as well as on Si surfaces coated with Al_2O_3 (Figure 1c) after methane CVD for 30 min. Transmission electronic microscopy results of samples with the same catalyst particles supported on alumina powder and treated with methane under the same conditions confirmed that the nanotubes observed with AFM are single-walled carbon nanotubes (Figure 1d).

It is interesting to find that individual SWNTs grown on Si surfaces take two perpendicular directions on Si(100), while on Si(111) they take one of the three directions separated by 60°. To determine the orientation distribution of the SWNTs on surfaces, we fixed the sample orientations when we imaged different areas on the same sample. The orientation histograms on these surfaces showed obvious discrete orientation distribution. We have observed the same orientation preference on several different surfaces, including Si surfaces with hydrogen passivation, Si surfaces with native oxide, and Si surfaces coated with ultrathin Al_2O_3 layers. These observations clearly reflect the influence of substrate lattices on the growth of SWNT in the methane CVD process.

To understand the observed orientation preference, we performed molecular simulation using empirical force potentials.¹³ The total interaction energy as a function of nanotube orientation and position on Si surfaces were examined for different tubes. For clarity, the unreconstructed Si(100) and Si(111) surfaces were used in the calculation. Figure 2 shows the total interaction energy as a function of the rotation angle between the tube axis and the silicon lattices (the data given are per length (Å) of the nanotube) for (10,10) and (18,0) tubes. Distinct orientational locking of SWNT with surfaces are clearly seen: locking orientations are separated by 90° on Si(100) and 60° on Si(111), reflecting the lattice symmetry of the substrates. In contrast to nanotubes on a graphite surface where orientational locking is chirality dependent,¹⁴ simulations show that orientational locking on Si surfaces is tube chirality independent, as observed in experiments. This agreement between theory and experimental observation indicates that it is energetically more favorable for SWNTs to grow along the directions defined by the underlying Si lattice to maximize the interaction between the tubes and the substrate. A possible mechanism is that at the initial stage of the growth, nanotubes have the mobility to rotate on surfaces due to thermal energy until they find the preferred orientations. For SWNTs grown on native oxide and ultrathin

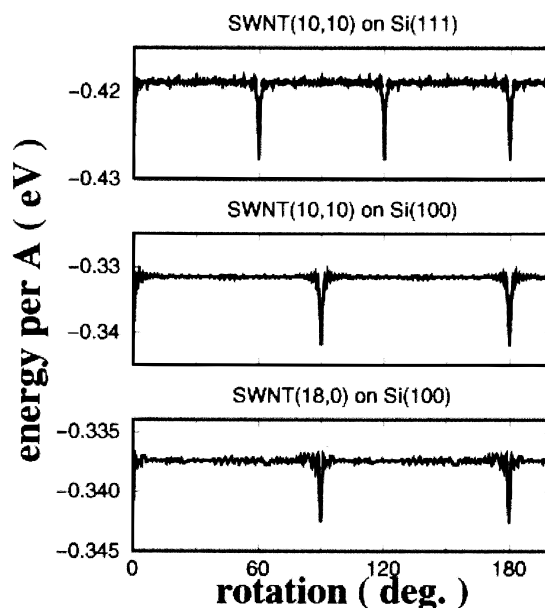


Figure 2. Interaction energy as a function of angle between the (10,10) tube axis and lattice on Si(111) (a) and Si(100) (b). (c) (18,0) on Si(100) shows the same orientational locking as the (10,10) tube.

Al_2O_3 layers, although the nature of the oxide and the Al_2O_3 layer is still not fully understood presently, it is clear that the symmetry of the underlying Si lattice is preserved.

Additionally, we have studied the same SWNT after different growth times to determine the growth mechanism of SWNT on a silicon surface. We first imaged an area with clear land marks, Figure 3a. Then the sample was put back into the CVD system for another 30 min. The AFM image of the same area after reaction, Figure 3b, showed that all nanoparticles did not change their positions and some SWNTs become longer. This observation unambiguously confirms the base-growth mechanism, in which the catalytic particles are stationary on the surface while the nanotubes grow away from the particles as they get longer. Another interesting observation we had is that the nanotubes grown on Si(100) are in general much longer than those on Si(111) grown under the same conditions. To explain this observation, we did simulation by moving a tube along the energy minimum direction. We found the energy barrier for sliding the tubes on Si(111) is 2 times higher than that on Si(100), Figure 4. This means the translation of SWNT on Si(100) is easier than that on Si(111) and may explain the fact that SWNT grown on Si(100) is longer than on Si(111) when the reaction conditions are the same.

We have noticed that not all nanoparticles deposited on the surface nucleate nanotubes. Actually, the yield of SWNTs is very low with respect to the total number of catalyst nanoparticles. Among all the studied systems, Fe on Si–H, Fe on SiO_2 , Fe–Mo on SiO_2 , Fe on Al_2O_3 , and Fe–Mo on Al_2O_3 , we have noticed that the SWNT yield of Fe–Mo composite particle on an Al_2O_3 monolayer is the highest. Not only the amounts of SWNTs are greater but also the lengths of individual SWNTs are longer. This observation is in good agreement with the results on the growth of SWNTs on catalysts supported on SiO_2 and Al_2O_3 powders.^{15,16,9} It strongly supports our hypothesis of “base-growth” mechanism, in which the catalyst particles have to attach strongly to the substrate in order to nucleate a nanotube. The interaction between the catalyst particles with the substrate plays a very important role in the growth process. The reason for the low yield of SWNT on Si and SiO_2 surfaces implies that the interactions with nanoparticles are not strong

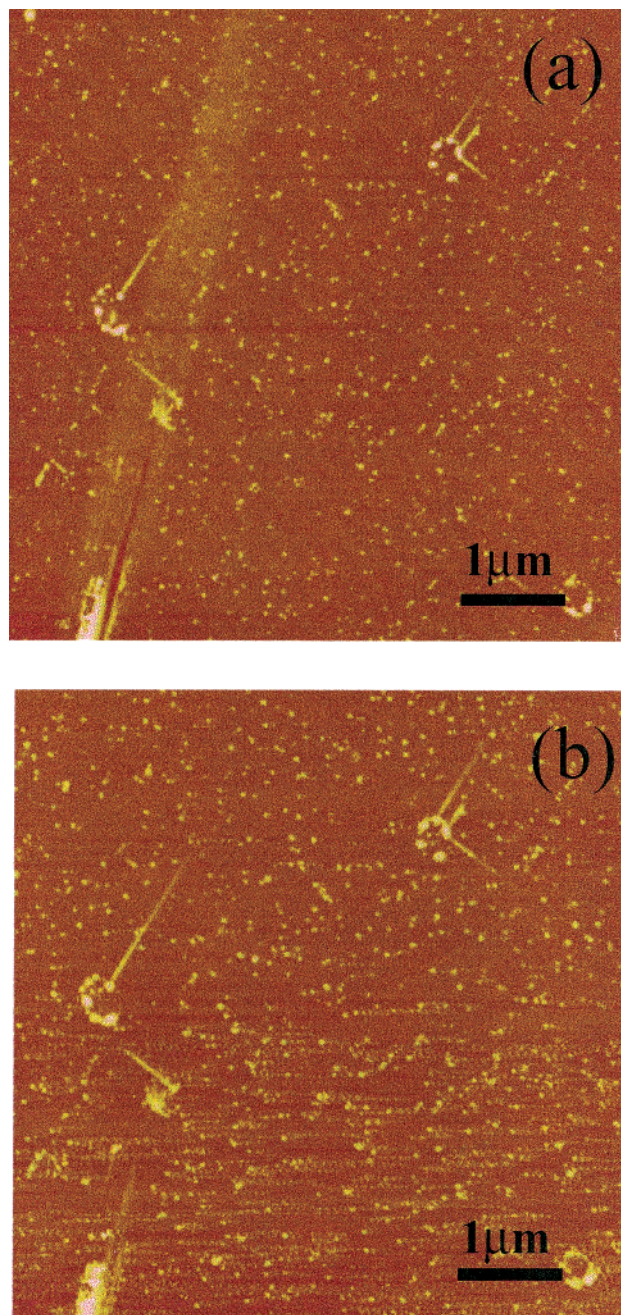


Figure 3. AFM images of the same area after CVD for 15 min (a) and another 30 min (b), confirming the base-growth of SWNT on surface.

enough unless the particles are adsorbed on certain defective sites. While on Al_2O_3 surfaces, pure Fe nanoparticles do not interact strongly with the surface but Fe—Mo alloy nanoparticles do. More works are underway currently focusing on further understanding of the interaction.

In summary, individual single-wall carbon nanotubes have been synthesized on surfaces from individual catalyst nanoparticles by chemical vapor deposition of methane. The SWNTs orient to certain directions on the Si(100) and Si(111) surface. Molecular simulations suggest that the SWNTs are guided by

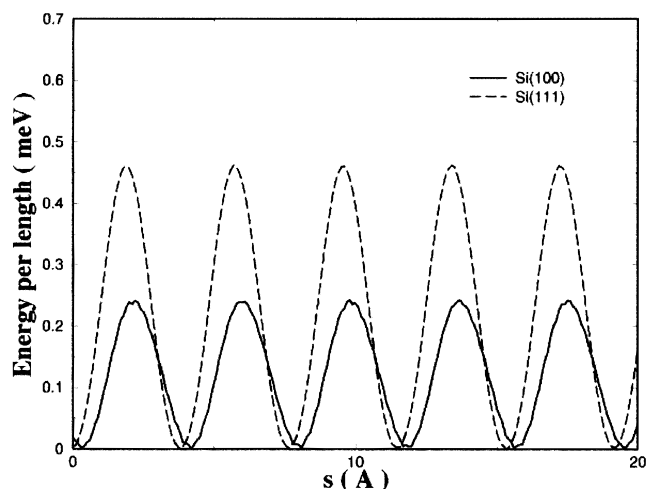


Figure 4. Comparison of energy barriers for sliding the (10,10) tube on Si(100) and Si(111) surfaces. The barrier (111) is twice of that on the (100) surface.

the surface lattice to follow a potential minimum path. The calculated orientation accords exactly with the AFM observed orientations of SWNTs. This lattice oriented growth of SWNT on surfaces enables us to have certain control over the orientation of nanotubes on surfaces, which is very important for the future fabrication of functional devices with nanotubes. We have also observed the growth of the same nanotube on the surface after different growth periods. This, together with the observation of importance of the substrate in nanotube growth, proved the growth mechanism of SWNTs in methane CVD is a “base-growth” mechanism.

Acknowledgment. This work is in part supported by Office of Naval Research grant no. 00014-98-1-0597 through UNC-CH.

References and Notes

- (1) Iijima, S. *Nature* **1991**, 354, 56–58.
- (2) Dresselhaus, M. S.; Dresselhaus, G.; Eklund, P. C. *Science of Fullerenes and Carbon Nanotubes*; Academic Press: San Diego, 1996.
- (3) Tans, S. J.; Verschuere, A. R. M.; Dekker, C. *Nature* **1998**, 393, 49–52.
- (4) Dai, H.; Kong, J.; Zhou, C.; Franklin, N.; Tomblor, T.; Cassell, A.; Fan, S.; Chapline, M. *J. Phys. Chem. B* **1999**, 103, 11246.
- (5) Tans, S. J.; Devoret, M. H.; Dai, H. J.; Thess, A.; Smalley, R. E.; Geerligs, L. J.; Dekker, C. *Nature* **1997**, 386, 474–477.
- (6) Lefebvre, J.; Antonov, R.; Johnson, A. T. *Appl. Phys. A (Mater. Sci. Processing)* **1998**, 67, 71–74.
- (7) Che, G. L.; Lakshmi, B. B.; Fisher, E. R.; Martin, C. R. *Nature* **1998**, 393, 346–349.
- (8) Li, W. Z.; Xie, S. S.; Qian, L. X.; Chang, B. H.; Zou, B. S.; Zhou, W. Y.; Zhao, R. A.; Wang, G. *Science* **1996**, 274, 1701–1703.
- (9) Kong, J.; Soh, H.; Cassell, A.; Quate, C.; Dai, H. *Nature* **1998**, 395, 878–81.
- (10) Hafner, J. H.; Cheung, C. L.; Lieber, C. L. *Nature* **1999**, 398, 761.
- (11) Ichinose, I.; Senzu, H.; Kunitake, T. *Chem. Mater.* **1997**, 9, 1296.
- (12) Martino, A.; Stoker, M.; Hicks, M.; Bartholomew, C. H.; Sault, A. G.; Kawola, J. S. *Appl. Catal. A* **1997**, 161, 235.
- (13) Casewit, C. J.; Rappe, A. K.; Colwell, K. S.; Goddard, W. A.; Skiff, W. M. *J. Am. Chem. Soc.* **1992**, 114, 10024.
- (14) Buldum, A.; Lu, J. P. *Phys. Rev. Lett.* **1999**, 83, 5050.
- (15) Su, M.; Zheng, B.; Liu, J. *Chem. Phys. Lett.* **2000**, 322, 321.
- (16) Cassell, A. M.; Raymakers, J. A.; Kong, J.; Dai, H. *J. Phys. Chem. B* **1999**, 103, 6484–6492.